PUBLIC HEALTH

Beyond the limit: The estimated air pollution damages of overshooting the temperature target

Clàudia Rodés-Bachs[1,2]*, Laurent Drouet[2,3], Peter Rafaj[4], Massimo Tavoni[2,3,5], Lara Aleluia Reis[2,3]

Exposure to outdoor air pollution results in millions of premature deaths and illnesses that are associated with substantial economic loss. According to the Global Burden of Disease, outdoor air pollution was responsible for 4.7 million deaths in 2021. Climate change mitigation policies could provide cobenefits by reducing air pollution. The Intergovernmental Panel on Climate Change AR6 report explores scenarios using an updated carbon budget approach—the net-zero pathways—designed to avoid temporary overshoot of the 1.5°C temperature limit. We assess whether net-zero pathways consistently improve air pollution outcomes using a global source-receptor air pollution model to estimate concentrations, health impacts, and economic damages. To analyze key uncertainties, we apply multiple relative risk functions and economic damage models. Our findings show that stringent climate policies, avoiding overshoot and keeping below 2°C, offer substantial health and economic cobenefits, particularly for China and India, and avoid 207,000 premature deaths and 2269 billion USD2020 in damages by 2030.

INTRODUCTION

Outdoor air pollution is the leading environmental health risk factor, responsible for more than 4.7 million premature deaths globally in 2021 (*1*, *2*). Beyond its mortality impact, outdoor air pollution is strongly associated with a broad spectrum of serious illnesses and economic losses (*3*–*7*). Many of these adverse outcomes can be mitigated through climate change policies because the reduction of greenhouse gas emissions not only addresses global warming but can also lower concentrations of harmful air pollutants, such as fine particulate matter ($PM_{2.5}$) and ozone (O_3). Therefore, climate mitigation policies have the potential to yield substantial cobenefits for air pollution reduction, resulting in substantial public health and economic advantages (*8*–*14*).

The latest generation of scenarios from the Intergovernmental Panel on Climate Change (IPCC) (AR6) (*15*) introduced an innovative approach to climate change mitigation: the global net-zero (NZ) pathways. These pathways, developed using integrated assessment models (IAMs), are primarily designed for evaluating mitigation strategies. Traditionally, these scenarios focus on the global cost-effectiveness of achieving a specific temperature target by the end of the century (*16*). However, this method can lead to overshooting trajectories (*17*), where global temperatures temporarily exceed the set limits before stabilizing at the target level. Addressing this overshoot requires a phase of net-negative carbon emissions in the latter half of the century to compensate for the initial exceedance (*18*). This approach not only heightens climate-related risks (*19*) but also depends heavily on the large-scale deployment of carbon dioxide removal (CDR) technologies (*20*, *21*).

Often, the IAMs used to project future climate scenarios do not explicitly account for air pollution. Thus, additional methods are required to estimate the effects of changes in levels of outdoor air pollution. This estimation involves a complex multistep process filled with various sources of uncertainty that can affect the projected impacts. When the air pollution impacts are reduced because of climate mitigation policies, they are referred to as cobenefits.

In this study, we investigate whether the climate policies aimed at avoiding temperature overshoot can consistently deliver robust air pollution cobenefits despite the uncertainties inherent in the estimation process. By systematically addressing these uncertainties, we aim to enhance the reliability of cobenefit projections and support the development of more effective and resilient climate policies.

Study design

We use a wide range of IAM emission scenario pathways, present in the AR6 database (*22*), and focus on 10 macroregions frequently used by the IPCC (see fig. S3 and table S1). The scenarios are produced by six IAMs: AIM CGE (*23*, *24*), IMAGE (*25*), MESSAGEix-GLOBIOM (*26*), POLES-JRC (*27*), REMIND-MAgPIE (*28*, *29*), and WITCH (*30*, *31*). These models are well established in evaluating global climate change mitigation pathways (*16*, *21*, *32*, *33*) and represent a broad spectrum of modeling approaches. Each model provides detailed representations of power and land-use systems and offers various decarbonization options. When used together, these models generate a comprehensive ensemble of pathways that capture a wide range of potential technological developments. This ensemble allows us to assess the robustness of the results and identify scenarios with significant "fat tail" risks, where the probability of extreme impacts is substantially higher than in a normal distribution (*19*, *34*).

We focus on the scenarios from the ENGAGE (Exploring National and Global Actions to reduce Greenhouse gas Emissions) project. Each model followed the same protocol to ensure comparability of results, as detailed in Methods and Riahi *et al.* (*21*). The models were designed to fit a carbon budget ranging from 200 to 3000 billion tonnes (Gt) of CO_2, which represents the cumulative CO_2 emissions from 2018 to 2100 aligned with specific long-term temperature targets for the two scenario designs. The end-of-century (EoC) pathway uses the carbon budget without restrictions, often resulting in delayed mitigation efforts and reliance on CDR technologies in the latter half of the century. This can lead to temporary temperature overshoot, which is later offset by net-negative emissions. In contrast, the NZ pathway uses the remaining carbon budget until CO_2 emissions are reduced to NZ. Once this target is achieved,

[1]Basque Center for Climate Change, Leioa, Spain. [2]CMCC Foundation–Euro-Mediterranean Center on Climate Change, Lecce, Italy. [3]RFF–CMCC European Institute on Economics and the Environment, Milan, Italy. [4]International Institute for Applied Systems Analysis (IIASA), 2361 Laxenburg, Austria. [5]Politecnico di Milano, Milan, Italy.
*Corresponding author. Email: claudia.rodes@bc3research.org

CO_2 emissions are maintained at zero, thus avoiding any overshoot and managing to prevent substantial temperature increases. The baseline scenario represents the continuation of current national policies up to 2100. The effects of the policy impacts are considered to occur in the same year as the reduction in emissions, aligning with the immediate nature of the policy interventions. Detailed scenario specifications are provided in Methods and Riahi *et al.* (*21*).

Our goal is to estimate the health and economic benefits of air pollution reduction in NZ pathways, accounting for the main sources of uncertainty. To achieve this, we identify these uncertainties throughout the multistep estimation process for air pollution cobenefits, illustrated in Fig. 1. This process starts with data acquisition from the ENGAGE scenario database (*35*), which provides air pollution emission data and other outputs from the IAM scenarios referenced above. Uncertainty stems from the choice of IAMs (*36*, *37*), as they each result in distinct pathways for air pollution emissions. Then, we use an R version of the TM5-FASST Scenario Screening Tool (TM5-FASST) (*38*) to estimate the concentrations of $PM_{2.5}$ and O_3 based on the emission data. These concentration estimates are crucial for assessing the health impacts. To ensure accuracy and minimize additional assumptions, we use the number of premature deaths associated with air pollution exposure—a direct and widely accepted metric for health impacts (*2*, *10*, *13*, *39*–*43*)—as our primary health-related measure. This metric relies on the relative risk (RR) value, commonly used to quantify the risk increase attributable to changes in pollutant concentrations. We consider uncertainties related to the choice and calibration of the RR function (*13*, *44*). Last, we estimate the economic damages resulting from the health impacts of air pollution. There are two main approaches to defining the economic damage function: one based on the number of premature deaths and the other on the concentration. Each approach introduces distinct uncertainties, which we account for in the final output (*45*). In addition, the parameters of the economic damage functions are derived from empirical studies that focus on a single macroregion and do not specifically apply to all global regions. To extrapolate these to other areas worldwide, we consider three different regional extrapolation parameters—low (0.8), medium (1), and high (1.2) income elasticities (details available in section S4).

To address the complexity and inherent uncertainty in model selection and function parameterization (*46*), we reviewed a broad array of functions and calibration values from the literature, as shown in Table 1. Although we are aware that some of these functions are more state of the art than others, all have been widely used at different points in time, and their inclusion allows us to better understand the evolution of the air pollution impact literature. In this study, we assessed the individual cobenefits associated with each uncertainty source, but for clearer presentation, we grouped the results into aggregated categories. Moreover, we organized the modeled carbon budgets into three distinct categories, detailed in table S2, recognizing the critical role of temperature in assessing climate impacts.

This article focuses on scenarios with carbon budgets below 1000 Gt of CO_2, which correspond to a global mean temperature increase of well below 2°C, unless otherwise noted. Figures corresponding to other carbon budget clusters are available in the Supplementary Materials. The reported values are provided as a range from minimum to maximum, covering all scenarios. This range includes variations in RR and economic damage functions, along with their parameters, unless otherwise specified.

To qualitatively assess the impact of pathway designs, such as NZ and EoC, under uncertainty, we use empirical probability distributions and cumulative probability functions. These statistical tools are effective in visualizing data distributions and estimating the likelihood of outcomes, which assists in understanding variability and assessing risks within the pathway scenarios. Moreover, we apply the nonparametric two-sided Kolmogorov-Smirnov test (*47*), which evaluates the likelihood that two sample sets originate from the same (but unknown) distribution. As further detailed in the "Policy design impact analysis" section, *P* values below 0.05 indicate that the two pathway designs have statistically different empirical probability distributions, demonstrating that the pathway choice substantially affects the output (i.e., emissions, concentrations, premature deaths, or economic impacts). In addition, we examine the probability of exceeding high mortality rates or economic cobenefits across climate pathways, highlighting low-probability but high-consequence scenarios. Last, we examine how outputs vary when all key parameters, counterfactual values, elasticity assumptions, and model choices are held constant, except for one.

RESULTS

Health cobenefits

In this study, we estimate premature mortality considering $PM_{2.5}$ adult-related deaths from ischemic heart disease, chronic obstructive pulmonary disease, lung cancer, and stroke, also called cerebrovascular disease, that comprehends ischemic stroke and hemorrhagic stroke (*3*, *42*, *48*); $PM_{2.5}$ children-related deaths from acute lower respiratory illness (*42*, *48*); and O_3 adult-related deaths from chronic obstructive pulmonary disease (*48*). All these impact metrics have mathematical

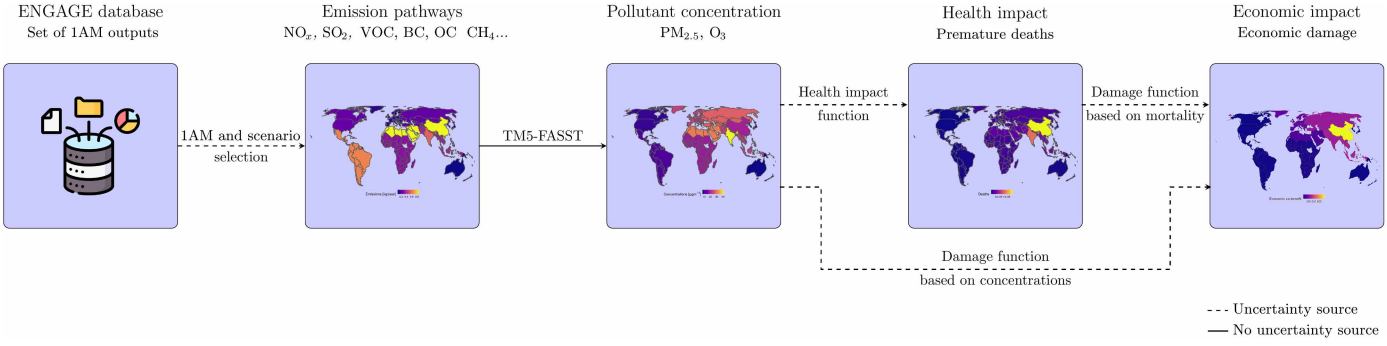

Fig. 1. Schematic workflow of the methodology.

Table 1. Details of the sources of uncertainty, options, and calibration settings.

Uncertainty source	Sensitivity
Air pollution emission's pathways	IAMs: AIM CGE, IMAGE, MESSAGEix-GLOBIOM, POLES-JRC, REMIND-MAgPIE, WITCH
	Scenarios
	Mitigation pathway: EoC (overshooting) or NZ (nonovershooting)
	Carbon budget: from 200 to 3000 Gt of CO2
	Short-term policy: current national policy or nationally determined contribution policy
Health impact function	RR function: GEMM, IER, log-linear
	Parameters of the RR function: described in Table S4
	Counterfactual value of the RR function: described in Table S4
Damage impact function	On the basis of pollutant concentration: Dechezleprêtre *et al.* (*58*) and Dong *et al.* (*59*)
	On the basis of premature mortality: VSL (*43*) and HCL (*60*)
	Elasticity value: high (1.2), medium (1), low (0.8)

forms that are based on the estimation of the RR. The formulation of the RR itself can take on different structures and includes several parameters and a counterfactual value, all of which contributes to the output uncertainty (*49*–*54*). In this study, we use parameters and counterfactual values from the literature, as detailed in table S4.

To see whether the two types of mitigation routes—EoC and NZ—are statistically different in terms of air pollution outcomes, we use the Kolmogorov-Smirnov two-sided statistical test (*47*) (fig. S4C). In line with previous studies (*19*, *21*), it shows that it is for more stringent scenarios (carbon budget < 1000 Gt of CO_2) where the mitigation route choice is more decisive. It is especially relevant for O_3 premature deaths, mainly driven by NO_x emissions, which are very responsive to the climate policy design (fig. S4A). For high carbon budgets, the mitigation design does not play any role. This can be seen in figs. S11 and S12, where the estimated premature deaths are not statistically different between the mitigation policy designs. This is explained by the fact that under mild climate policies, the energy system is left with more technology options as the global carbon tax is less extreme. This gives more room to fulfill carbon budgets and allows for the deployment of advanced technological alternatives later in the century. Similar results were found for climate risks (*19*). Here, we focus on 2030 not only for its policy relevance but also because it represents the point of greatest divergence between NZ and EoC and thus a higher impact (see section S5 for further details and an analysis of the year 2050). This happens because avoiding overshoot of temperature anticipates climate mitigation, thereby yielding greater air pollution benefits in the early years.

Analyzing the regional distribution of health cobenefits from reduced temperature overshoot, as shown in Fig. 2A, we find that China and India experience the greatest reduction in air pollution–related premature mortality following the NZ pathway rather than the EoC pathway, the estimated reductions in premature deaths by 2030 are 84,000 (ranging from 40 to 144,000) in China and 73,000 (ranging from 43,000 to 111,000) in India, as depicted in Fig. 2A. This finding emphasizes two crucial points: (i) The effectiveness of global climate policies heavily depends on these two major developing economies to decarbonize; (ii) these regions, potentially through funding provided by the sixth article of the Paris Agreement, have the opportunity to reduce their carbon emissions and simultaneously reap health benefits from improved air quality.

As shown in Fig. 2B, the estimated premature deaths vary depending on the chosen RR function, its parameters, and the counterfactual values used for calibration. Nevertheless, the NZ pathway consistently dominates the EoC, shifting the empirical cumulative distribution function (eCDF) estimates to the left in both 2030 and 2050 (Fig. 2C and figs. S11 and S12), i.e., delivering consistently less premature mortality. This pattern holds across all normative assumptions, with the NZ pathway reliably delivering lower mortality estimates (further details in section S10).

When evaluating the main contributors to uncertainty in premature death estimates from air pollution, our analysis, as illustrated in Fig. 3 (A and B), examined the contributions of each factor. We identified two distinct regional groups, each affected differently by these sources of uncertainty. The first group consists of Europe, Latin America, North America, Pacific-OECD, and reforming economies (regions' details in table S1), which are generally high- to medium-income countries. In these regions, the primary source of uncertainty is sensitivity to parameter choices, as illustrated in Fig. 3A. This is evident from the greater difference between medians (represented by bullets) of the same color compared to those with the same line type, indicating that parameter selection plays a substantial role in driving uncertainty. The second group includes Africa, China, India, the Middle East, and the rest of Asia (regions' details in table S1), which are primarily low- to medium-income countries with larger populations. Here, the primary source of uncertainty is the counterfactual value, which determines the threshold at which air pollutants are considered harmful. This is shown in Fig. 3B, where the difference between medians with the same line type is more pronounced than between medians with the same color. This indicates that variations in the counterfactual value contribute more to the overall uncertainty, particularly in densely populated regions (further details in section S11).

Another substantial source of uncertainty arises from the emission pathways estimated by the IAMs, as shown in Fig. 3C. This figure displays the empirical probability density distribution function for each IAM considering the various RR functions with their parameters

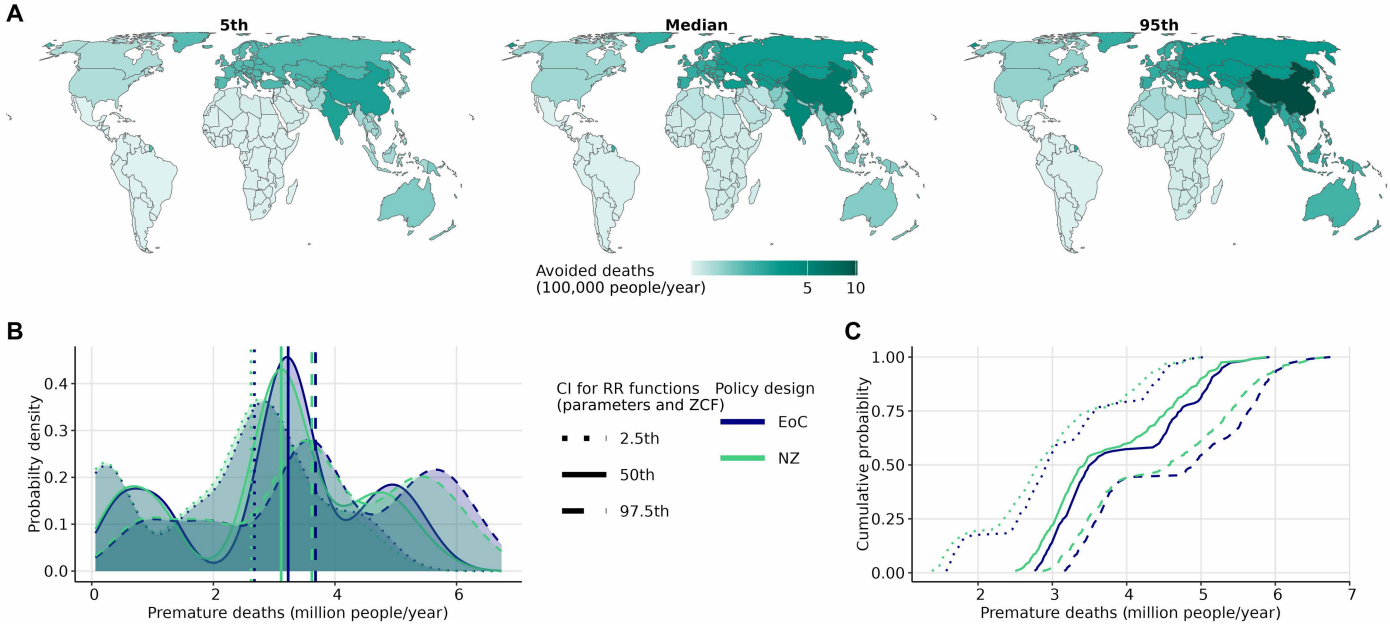

Fig. 2. Global health cobenefits of reduced overshoot for the year 2030. The distribution ranges include the various RR functions, their parameters and counterfactual value ranges, and the various emission pathways generated by the IAM scenarios. The green and blue colors indicate the policy design (EoC or NZ). The line type distinguishes the confidence interval (CI) percentile generated by combining the RR functions with their different parameters and counterfactual values (ZCF). (**A**) Estimated 2.5th, 50th, and 97.5th percentiles of avoided premature deaths per 100,000 population, normalized when following the NZ mitigation pathway instead of the EoC pathway. (**B**) Empirical probability density functions (ePDFs) of the estimated premature deaths expressed in millions of people. The vertical dashed line indicates the median. (**C**) Empirical cumulative probability functions of the estimated premature deaths expressed in millions of people.

and counterfactual values set to the median. The distribution of avoided deaths under nonovershooting temperature policies shows consistent shapes and median values, ranging from 3.13 to 3.77 million, across the different IAMs. In contrast, Fig. 3D highlights the empirical probability density functions (ePDFs) for the various RR functions applied to the emission pathways generated by the IAMs. Here, the estimated medians vary substantially across the RR functions, ranging from 2.84 to 5.05 million, and the shapes of the ePDFs differ as well. This indicates that when estimating the health impacts of air pollution, the choice and calibration of the RR function are more critical than the choice of the IAM. Further details on the sources of uncertainty and how they propagate are provided in section S6.

Figure 3D also captures the progression of RR functions throughout time. The integrated exposure-response (IER) function [Burnett *et al.* (*50*) and GBD in 2015 (*55*)] exhibits low tails and estimates. However, when using the more recent RR functions [Burnett *et al.* (*49*)] following the Global Exposure Mortality Method (GEMM), the estimates and tails increase sharply. This helps to interpret the difference in the outcomes of some health impact studies performed during those years. All the functions and their parameters for the different cohorts (e.g., low, medium, high, with, and without) are detailed in section S3 and summarized in table S4.

Last, we investigated the probability of exceeding "high" mortality rates and conducted empirical tests to determine whether these probabilities differ between the NZ and EoC pathways, following the approach outlined in (*19*). Given the lack of observations in our case, we defined the high value as the 90th percentile of premature mortalities under the NZ pathway over the century. This threshold helps to understand how the exceeding probability evolves over time. Our findings indicate that NZ policies considerably reduce the likelihood of extremely high premature death estimates across all regions, making these outcomes less probable (extended details in section S7). However, an exception exists with the IER function, where both EoC and NZ policies yield similar results. This is due to a constant counterfactual factor in the IER function, which makes the results less sensitive to concentration changes compared to the other functions considered in this study. Further details on the RR functions are provided in the "Premature mortality" section and section S3.

Economic cobenefits

Previous literature has extensively analyzed the macroeconomic long-term impacts of climate change (*56*, *57*). The projections are very sensitive to the considered methods and assumptions, and there are clear methodological limitations to quantify climate-related economic damages. Thus, the economic evaluation should only be used to enhance the health impact study, as in (*19*). Here, we considered four different methods to estimate the economic damages of air pollution. Two of these methods correlate gross domestic product (GDP) with air pollution concentrations, proposed by Dechezleprêtre *et al.* (*58*) and Dong *et al.* (*59*). The other two methods rely on premature mortality data: the value of statistical life (VSL) (*43*) and the human capital loss (HCL) (*60*). Consequently, these latter two methods—the VSL and the HCL—are susceptible to the uncertainties inherent in estimating premature deaths (as detailed in the "Economic damages" section and section S4). None of these functions account for reduced pollution control costs, meaning that they do not explicitly include policy costs in their equation. However, the costs associated with reduced overshoot are implicitly captured in the IAMs' GDP

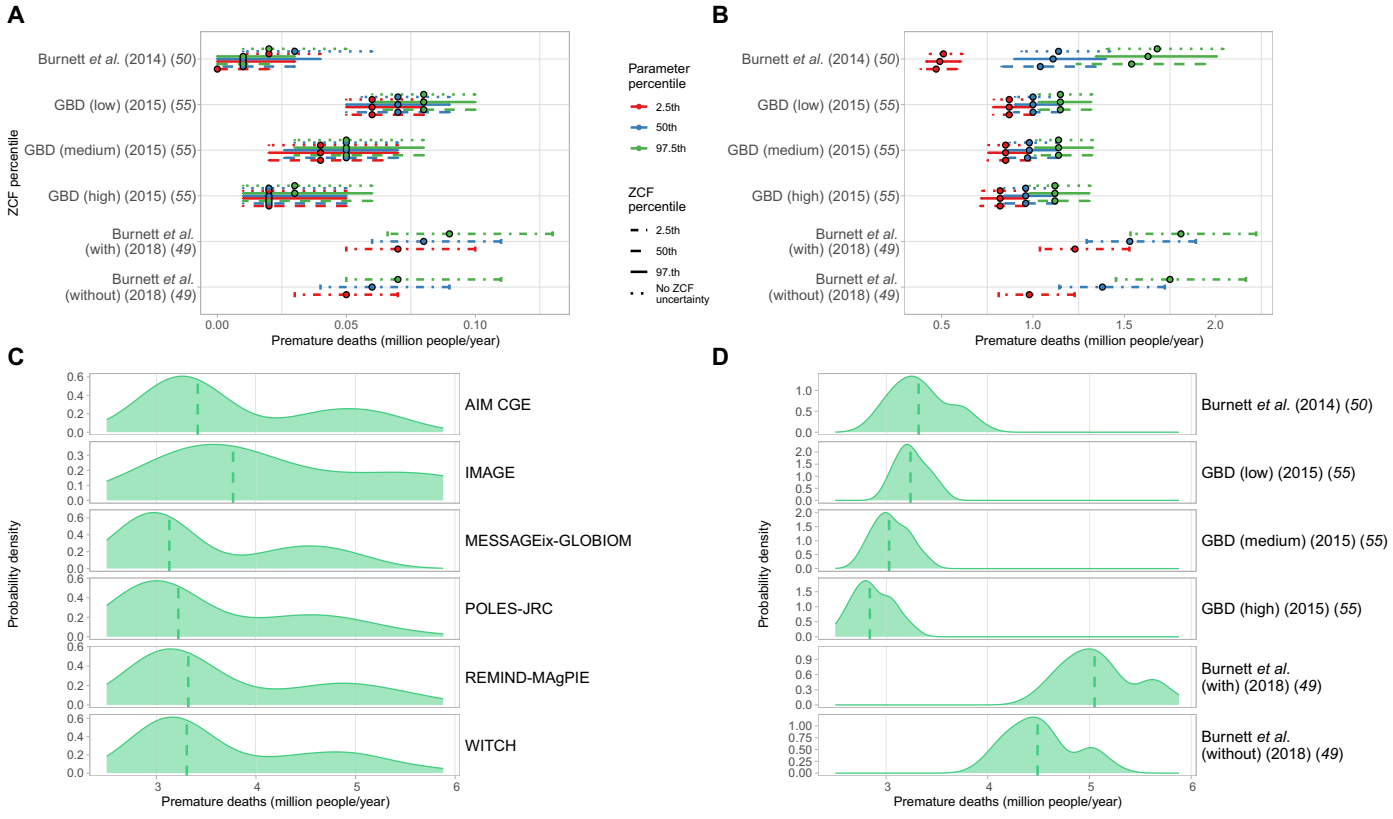

Fig. 3. Health cobenefits uncertainty for the year 2030 when following the NZ policy design. Data are expressed in millions of people. (**A** and **B**) Uncertainty interval of the estimated premature deaths (2.5th to 50th to 97.5th percentile range) driven by the RR functions' parameters, indicated with the color, and the RR functions' counterfactual value, indicated with the line type. The representative regions are (A) North America and (B) China. The distribution ranges include the various RR functions, the multiple emission pathways generated by the IAM scenarios, and either the parameters or the counterfactual value range. (**C** and **D**) Empirical probability density distribution functions of the estimated premature deaths by (C) IAM and (D) RR function. The vertical dashed line represents the median. The distribution functions are set over the median counterfactual and parameters values of the RR functions.

projections. As a result, the HCL and Dong *et al.* (*59*) methods indirectly account for mitigation costs because their calculations explicitly include GDP or GDP growth in their formulas.

Applying the same analytic methods as for the health impacts, we find that the NZ policy design delivers consistently more cobenefits in all regions relative to the EoC design, not only for more stringent carbon budgets but also for medium carbon budgets, because the *P* values of the Kolmogorov-Smirnov test are under the significance level (fig. S4D). China experiences the major economic cobenefits, avoiding 922 billion USD2020 (range 849 to 1077 billion) in 2030 and 383 billion USD2020 (range 366 to 766 billion) in 2050, when following the NZ mitigation pathway instead of the EoC pathway (Fig. 4A and fig. S14). All regions, except Latin America, benefit from the NZ policy design despite the uncertainty range in the elasticity values. The elasticity value has only a small impact (globally) on the total avoided economic damage, and it does not affect the heaviness of the tails (Fig. 4, B and C). The negative impact that Latin America experiences happens in 2050 when using the economic damage function of Dechezleprêtre *et al.* (*58*) with medium elasticity (fig. S14). This occurs because the NZ policy design is more costly than that of the EoC, resulting in a lower per capita income in NZ. This results in fewer health benefits under the NZ pathway compared to the EoC pathway, as the impact of air pollution is estimated by extrapolating from this lower per capita income. It is also worth noticing that Latin America has one of the lowest air pollution reduction due to decarbonization (Fig. 4A).

The VSL method appears to be considerably more sensitive to variations in the RR function compared to the HCL. This is evidenced by the stability of the median and the 2.5th to 97.5th percentile range across different concentration-response functions, as shown in Fig. 5 (A to D). This occurs because the HCL method considers the years of life lost, while the VSL approach assigns a single value to the loss of life, regardless of when it occurs. Moreover, the VSL method is substantially influenced by regional elasticity assumptions, which causes a wide variation in the uncertainty range based on the chosen elasticity values, as depicted in Fig. 5 (A to D). This variability underscores how heavily the economic impact assessments of air pollution reduction policies depend on the relationship between air pollution and per capita income, as modeled by the VSL.

The response to VSL elasticity varies by region. Most regions show a direct correlation with the elasticity values, i.e., increasing elasticity values leads to increasing cobenefits. The exceptions are Africa, India, reference economies, and the rest of Asia. In these regions, the response is inverse because their per capita incomes in future years are lower than the OECD calibration value used for VSL calculations (as detailed in sections S4 and S13). Apart from the VSL

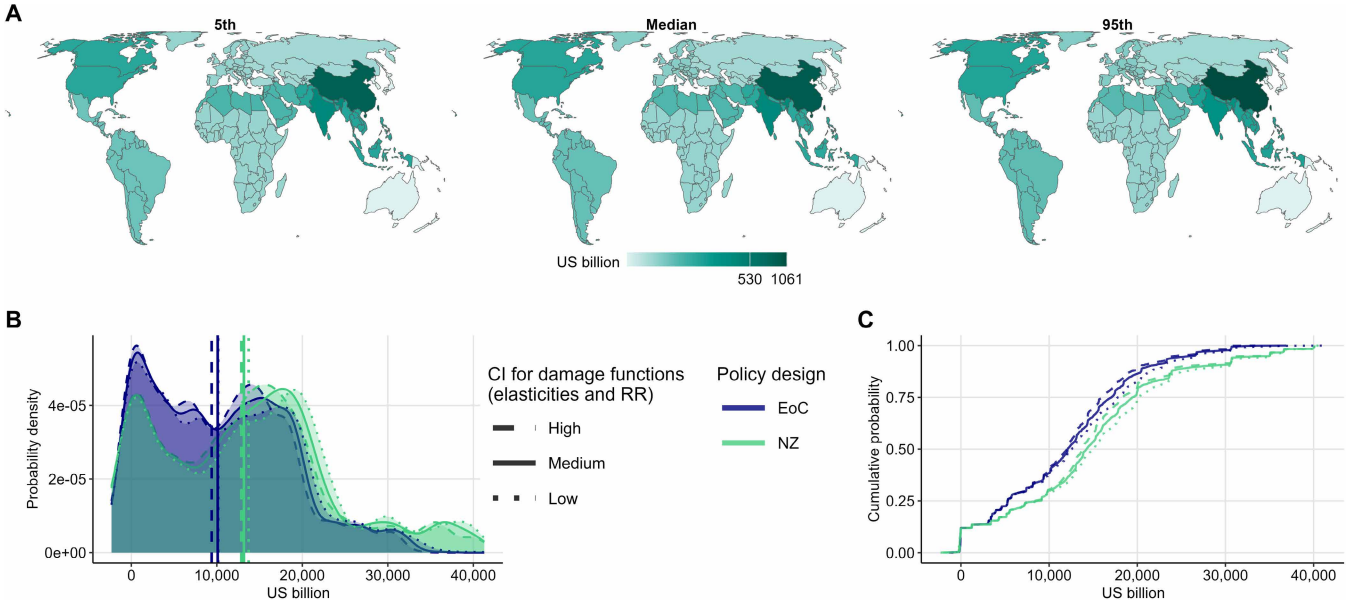

Fig. 4. Global economic cobenefits of reduced overshoot for the year 2030. Data are expressed in billion USD2020. The distributional ranges include the various economic damage functions with their various elasticity values, the various RR functions with their parameters and counterfactual value ranges, and the various emission pathways generated by the IAM scenarios. The green and blue colors indicate the policy design (EoC or NZ). The line type distinguishes the elasticity value choice (low, medium, and high) of the economic damage functions. (**A**) Estimated 2.5th, 50th, and 97.5th percentiles of economic cobenefits when following the NZ mitigation pathway instead of the EoC pathway. (**B**) ePDFs of the estimated economic cobenefits. The vertical lines represent the median. (**C**) Empirical cumulative probability functions of the estimated economic cobenefits.

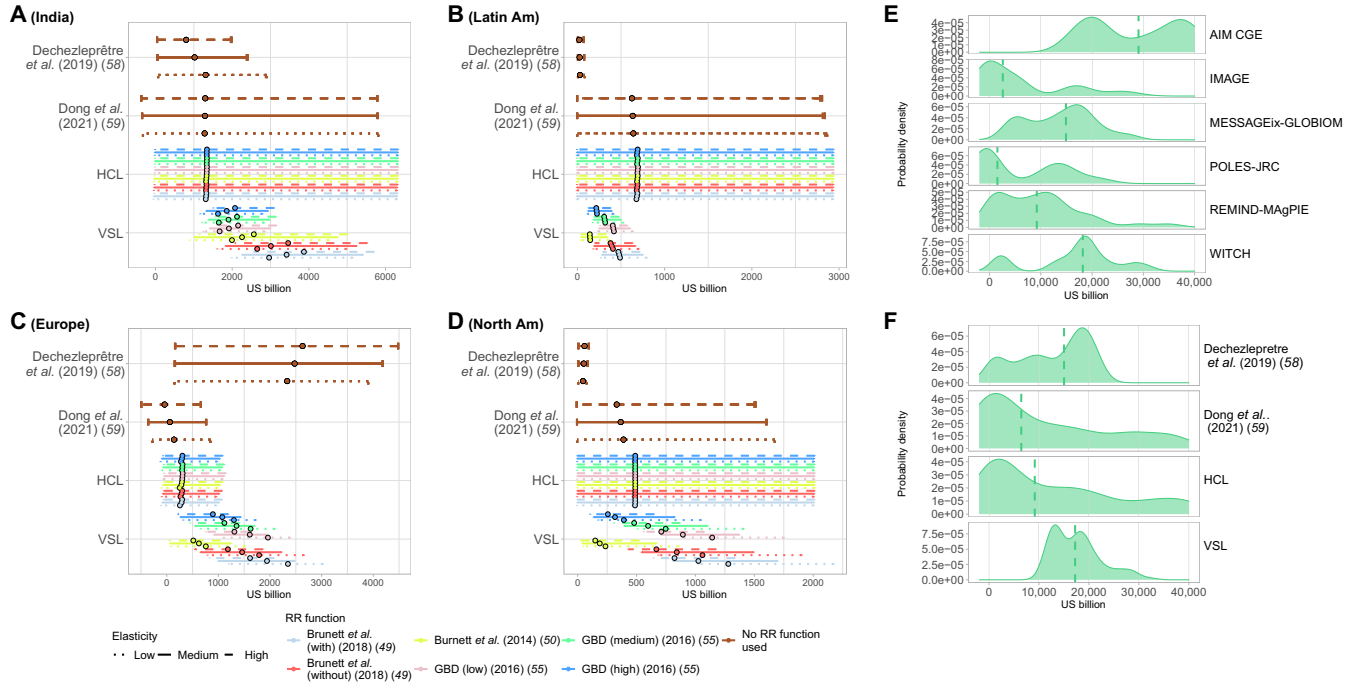

Fig. 5. Economic cobenefits uncertainty for the year 2030 following the NZ policy design. Data are expressed in billion USD2020. (**A** to **D**) Uncertainty intervals of the estimated economic cobenefits (2.5th to 50th to 97.5th percentile range) per economic damage function driven by the RR function, indicated with the color, and the elasticity value, indicated with the line type. The representative regions are (A) India, (B) Latin America, (C) Europe, and (D) North America. The distribution ranges include the various emission pathways generated by the IAM scenarios and either the economic damage functions, the RR functions with their parameters and counterfactual value variability, or the elasticity value of the economic damage functions. (**E** and **F**) Empirical probability density distribution functions of the estimated avoided economic damages by each (E) IAM and (F) economic damage function. The vertical dashed line represents the median. The distribution functions are set over the median counterfactual and parameters values of the RR functions.

method, the HCL, Dong *et al.*, and Dechezleprêtre *et al.* methods demonstrate robustness in their estimations of the economic cobenefits, as evidenced by stable median values and 2.5th to 97.5th percentile ranges across various elasticities and RR functions (Fig. 5, A to D).

Figure 5E illustrates the empirical probability distribution of economic cobenefits for each IAM, considering (i) the four economic damage functions, (ii) the various RR functions with their parameters and counterfactual value set to the median, and (iii) the different elasticities. The distribution of cobenefits from nonovershooting temperature pathways varies substantially across models, with different shapes and median values ranging from 1531 to 29,057 billion USD2020, with the AIM CGE model showing the highest economic cobenefit. In contrast, Fig. 5F displays the empirical distribution functions for economic cobenefits across the different economic damage methods, considering (i) the various integrated assessment emission scenarios, (ii) the various RR functions with their parameters and counterfactual value set to the median, and (iii) the varying elasticities. The median estimated economic cobenefit of the NZ policy design across these damage functions falls within a narrower range of 6457 to 17,237 billion USD2020, with the Dong *et al.* method providing the lowest estimate and the VSL method the highest. Thus, despite the large tails in the distributions for the HCL and Dong *et al.* methods, the primary source of uncertainty in estimating economic damages is identified as the IAMs. Further details on this are provided in section S6.

A closer look at the empirical probability density of the HCL and Dong *et al.* economic damage functions reveals that their shapes are quite similar. Both methods estimate avoided economic damage by considering the cost of mitigation, using GDP estimates from IAMs that incorporate climate mitigation costs. In these approaches, the design of the climate mitigation policy—NZ or EoC—not only reduces mortality due to air pollution but also lowers the magnitude of the parameters in the economic impact function. Specifically, in the Dong *et al.* methodology, the reduced GDP from mitigation costs leads to a decrease in the parameter that influences GDP growth due to air pollution. Similarly, for the HCL method, lower GDP due to mitigation costs results in reduced income levels, which, in turn, lowers the HCL. This method differentiates by age, incorporating remaining life expectancy across population groups, whereas the other three methods apply a single value per region, irrespective of age demographic differences. On the other hand, the economic damage avoided through the VSL and Dechezleprêtre *et al.* methods accounts for the impact of air pollution on GDP but does not consider the cost of mitigation in any form. Detailed descriptions of these methods can be found in section S4.

Last, using the exact Pearson-Klopper method (detailed in the "Tail heaviness analysis" section) with the 90th percentile of economic cobenefits under the NZ pathway as the threshold for high values, we observe that the NZ policy design results in heavier tails, indicating a higher likelihood of substantial economic cobenefits compared to the EoC policy design. This effect is particularly pronounced when applying the HCL or Dong *et al.* functions, as detailed in section S7. The limited observations necessitate this approach, but the findings underscore the greater potential for substantial cobenefits under the NZ pathway.

DISCUSSION

The analysis presented here has explored the health and macroeconomic impacts of outdoor air pollution of the latest generation of IPCC climate mitigation pathways. This work enlarges the results found by Drouet *et al.* (*19*) by providing a thorough analysis of the health and economic damages and risks of air pollutants when overshooting the temperature target.

While several studies have examined the effects of nonovershooting scenarios, most have overlooked the regional impacts of outdoor air pollution and the uncertainties inherent in their estimation. In this work, we address these gaps by incorporating a broad range of uncertainties in estimating health and economic damages across future scenario pathways. The large scenario ensemble used in this study strengthens the robustness of the results, demonstrating that the advantages of nonovershooting pathways remain consistent across various uncertainty factors such as the models, functions, or calibration values applied in the estimation process. Our findings highlight the importance of the scenario design in shaping effective mitigation policies. These decarbonization strategies can not only curb global warming but can also offer substantial cobenefits, in particular improved public health and enhanced economic prosperity.

Although multimodeling studies are recurrent in the IAM literature (*61*, *62*), to the best of our knowledge, no previous studies have considered such a wide range of computational methods to estimate premature mortality and economic damages. This analysis proves that anticipating mitigation efforts through nonovershooting scenarios benefits both the near future (2030) and mid-century (2050), which is in line with previous research (*19*, *21*). In terms of health cobenefits, it reduces the expected premature mortalities and lowers the probability of high mortality outcomes. From the economic point of view, it reduces the economic cost of air pollution and increases the probability of high economic cobenefits. The sensitivity analysis demonstrates that health estimates related to air pollution are highly influenced by the choice of the RR function, underscoring the need for substantial advancements in this area. Notably, the key sources of uncertainty within these functions vary by region, with distinct patterns emerging between low- and middle-income regions versus higher- and middle-income regions. In contrast, economic damage estimates are more sensitive to the selection of the IAM because these models have strong assumptions about air pollution policies, technology portfolios, and methods for calculating GDP losses. These findings emphasize the critical importance of further research into the spatially detailed income effects and distributional impacts of air pollution, particularly in developing countries.

Our results show that China and India stand to gain the most from nonovershooting climate policies. These policies require substantial reductions in greenhouse gas emissions from these regions, leading to substantial cobenefits in terms of air pollution reduction, fewer premature deaths, and lower economic losses. At the same time, these countries face important equity challenges. While they contribute a large share of current global emissions, they also endure some of the highest health burdens from air pollution (*5*, *63*, *64*). However, their historical responsibility for climate change remains lower than that of developed nations. Allocating mitigation efforts based on historical responsibility could help distribute costs more fairly while still delivering substantial air pollution benefits in these highly affected regions. Mechanisms such as funding through article 6 of the Paris Agreement (*65*) could provide much-needed financial and technological support, helping them transition to cleaner energy sources while improving air quality. This dual benefit would not only mitigate environmental and health disparities but also promote a more just and equitable shift toward a low-carbon future.

The modeling framework used in this study has some limitations that can be addressed in future research. The considered scenario ensemble considers more restrictive carbon budgets for overshooting pathways than for nonovershooting pathways (details in table S3), which might lead to somewhat conservative results. Although we consider various sources of uncertainty, we did not include in this analysis the uncertainty and sensitivity of the air pollution model selection and the baseline mortality estimates. Future updates to the model will incorporate the most recent datasets as they become available. According to literature sources (*1*, *66*), these updates are expected to increase premature death estimates, as recently available data indicate rising baseline mortality rates in almost all regions. Similarly, the scope of diseases considered could be expanded to include conditions such as lower respiratory infections in adults and diabetes, potentially leading to higher estimates of premature mortality. Furthermore, methodological differences in economic loss estimation from air pollution play an important role in generating heavy tails and uncertainty, as discussed in section S4. Last, we did not include MR-BRT (meta-regression–Bayesian, regularized, trimmed) mortality functions used in recent GBD studies (*67*) due to constraints in deriving their parameters. However, the existing literature (*5*, *68*, *69*) suggests that estimates based on the adoption of MR-BRT yield substantially lower mortality impacts than earlier IER and GEMM functions. This discrepancy stems from differences in the pollution sources and disease categories accounted for in the calibration of these functions. Future research could further investigate the implications of these functions and their underlying assumptions for macroeconomic impact assessments.

Despite its limitations, this study offers timely and valuable insights for both the scientific community and global and regional stakeholders. While air pollution damages are not systematically considered in most IAM-based studies, our findings demonstrate that their inclusion can considerably influence results, which can be sensitive to both the mitigation policy pathway and the computational assumptions used. Incorporating human health and economic impacts into climate policy design could have influenced the outcomes of previously published research. Air pollution, recognized as the leading environmental health risk by multiple institutes and global studies (*70*, *71*), is a critical factor in this context. Our results contribute to this literature, emphasizing the need for mitigation policies that not only address global warming but also enhance public health and economic well-being. To produce reliable and precise estimates, our study highlights the necessity of refining estimation methods to account for the unique circumstances and specific regional conditions. Future research could also consider including both climate and air pollution damages for a fully integrated assessment of cobenefits and/or cross-benefits.

MATERIALS AND METHODS

The workflow undertaken in this study is summarized in Fig. 1.

Model scenarios

For this analysis, we consider the outputs of six IAMs from the ENGAGE project database (*35*) with enough pollutants to estimate the concentrations of $PM_{2.5}$ and O_3: AIM CGE (*23*, *24*), IMAGE (*25*), MESSAGEix-GLOBIOM (*26*), POLES-JRC (*27*), REMIND-MAgPIE (*28*, *29*), and WITCH (*30*, *31*). Using two climate policies—EoC, which allowed for temperature overshoot, and NZ, which did not—these models produced emission trajectories compatible with a wide variety of carbon budgets (i.e., cumulative CO_2 emissions). Each modeling team followed the same protocol to ensure comparative results. Models also implemented country-specific current regulations, such as carbon fees, restrictions on fossil fuels, standards for renewable energy sources, etc. The COVID-19 pandemic's impact is not accounted for in this study. The NPi2100 is considered as the reference scenario, which represents the continuation of the current national policies up to 2100. For further details, see table S3.

From these models, among other outputs, we consider emissions from eight pollutants that contribute to the formation of $PM_{2.5}$ and O_3: BC, OC, NO_x, SO_2, CO, CH_4, NH_3, and VOC. All the impacts are computed by the R10 regions' cluster: Africa, China, Europe, India, Latin America, the Middle East, North America, Pacific-OECD, reforming economies, and the rest of Asia (fig. S3 and table S1). The modeling procedure and the model scenarios are fully described by Riahi *et al.* (*21*).

$PM_{2.5}$ and O_3 concentrations

To estimate the concentrations of $PM_{2.5}$ and O_3 from the emissions provided by the ENGAGE scenario database, we use an R version of the TM5-FASST Scenario Screening Tool [TM5-FASST] (*38*). It is a global reduced-form air quality source-receptor model from the TM5 chemical transport model that makes use of precomputed emission-concentration transfer matrices between pollutant source regions and receptor regions. These matrices emulate underlying meteorological and chemical atmospheric processes for a predefined set of meteorological and emission data and have the advantage that concentration responses to emission changes are obtained by a simple matrix multiplication, avoiding expensive numerical computations (*38*). In particular, we obtain the $PM_{2.5}$ annual average daily exposure and the O_3 seasonal—both 6- and 3-month—hourly maximum concentrations, as in (*38*). For further details, see section S3.2 and the model's reference paper (*38*).

Premature mortality

The premature deaths are estimated from $\Delta\mathrm{Mort} = y_0 \cdot \mathrm{PAF} \cdot \mathrm{pop}$, where y_0 is the cause-specific baseline mortality, pop is the exposed population, and PAF is the population-attributable fraction. This last item is based on the RR value, which can be computed through different RR functions. In this study, we consider RR functions used in the past decade in outdoor air pollution studies, being different IER functions [published by Burnett *et al.* (*50*) and the GBD in 2015 (*55*)] and various GEMM functions [published by Burnett *et al.* (*49*)] for $PM_{2.5}$ and two log-linear functions [published by Jerrett *et al.* (*41*) and the GBD in 2015 (*55*)] for O_3. Each literature source provided the global calibration parameters and, in some cases, also defined the uncertainty range (details in table S4).

Our calculation of premature mortality has a limitation: It does not account for the potential reductions in mortality that the policy itself might generate, as suggested in (*72*). This oversight could lead to an underestimation of the policy's benefits because the policy could increase both the proportion of elderly individuals and the total population size. For further details on the RR functions, mortality baselines, age stratification, and spatial scales, see section S3.

Economic damages

This study uses four different methods to estimate the economic damage of air pollution: the well-known VSL (*43*), two causal estimation methods based on empirical models, suggested by Dong *et al.* (*59*)

and Dechezleprêtre *et al.* (*58*), and the HCL (*60*). Because the last three methods were designed using only $PM_{2.5}$ data, we only estimate the $PM_{2.5}$ avoided economic damage, i.e., the economic gain derived from applying climate policies—NZ or EoC—relative to the reference. To see the damage functions and further analysis, see section S4.

Policy design impact analysis

To study how the climate policy design—NZ or EoC—affects the premature deaths or the economic damage estimates, we rely on different statistical methods. First, we use the ePDF and the eCDF. The former shows the likelihood of obtaining a given value for a variable of interest, in our case, the estimated premature deaths or the economic damage. By analyzing the ePDF shapes by climate policy design, we can identify which policy design predicts higher values for our variables, often using the median for simplicity. Moreover, the qualitative analysis of the ePDF is used to discuss the tail heaviness. To complement the ePDF analysis, we use the eCDF. The eCDF is a useful tool for analyzing differences between the distributions of the NZ and EoC policy design outcomes. For instance, if the eCDF of premature mortality under the NZ policy design is consistently to the left of that under the EoC policy design, then it indicates that, for the same probability, the NZ policy design consistently predicts lower premature mortality. Furthermore, considering the eCDF function by elasticity value or confidence interval (CI) percentile of the RR functions' parameters allows us to analyze the impact of these choices on the final output. This can be done by observing the relative position of the eCDF functions and their different slopes. Detailed figures for all regions, years, and scenario groups can be found in sections S8 to S10 and S12. Second, we considered the Kolmogorov-Smirnov two-sample test to quantify the difference between climate policies. As further detailed in section S5, if the P value exceeds 0.05, we accept the null hypothesis, indicating that both empirical distribution functions (with and without overshooting) originate from the same data and are statistically indistinguishable.

Uncertainty analysis

Several sources of uncertainty are taken into account: the uncertainty associated with emissions, derived by the range of IAMs; the uncertainty associated with the premature mortality estimates, derived by the RR functions and their parameters and counterfactual values; and the uncertainty associated with the economic damages of air pollution, derived by the economic methods and their elasticity values. Figure S5 lists these sources of uncertainty and provides a representation of the uncertainty propagation. Moreover, in section S6, we detail the uncertainty contribution of each source and the uncertainty propagation.

Tail heaviness analysis

Statistical tests are conducted to assess the likelihood of heavy tails in the ePDFs of premature mortality and avoided economic damages. This type of analysis is relevant for understanding the policy risks associated with extreme undesirable outcomes (e.g., very high mortality). In section S7, the method and assumptions for the tail heaviness analysis are described in great depth.

Supplementary Materials

This PDF file includes:

Supplementary Text
Figs. S1 to S15
Tables S1 to S4
References

REFERENCES AND NOTES

1. GBD 2021 Risk Factors Collaborators, Global burden and strength of evidence for 88 risk factors in 204 countries and 811 subnational locations, 1990–2021: A systematic analysis for the Global Burden of Disease Study 2021. *Lancet* **403**, 2162–2203 (2024).
2. Health Effects Institute, "State of global air 2024" (Special Report, Health Effects Institute, 2024).
3. X. Bu, Z. Xie, J. Liu, L. Wei, X. Wang, M. Chen, H. Ren, Global PM2.5-attributable health burden from 1990 to 2017: Estimates from the global burden of disease study 2017. *Environ. Res.* **197**, 111123 (2021).
4. R. T. Burnett, J. V. Spadaro, G. R. Garcia, C. A. Pope, Designing health impact functions to assess marginal changes in outdoor fine particulate matter. *Environ. Res.* **204**, 112245 (2022).
5. A. Pandey, M. Brauer, M. L. Cropper, K. Balakrishnan, P. Mathur, S. Dey, B. Turkgulu, G. A. Kumar, M. Khare, G. Beig, T. Gupta, R. P. Krishnankutty, K. Causey, A. J. Cohen, S. Bhargava, A. N. Aggarwal, A. Agrawal, S. Awasthi, F. Bennitt, S. Bhagwat, P. Bhanumati, K. Burkart, J. K. Chakma, T. C. Chiles, S. Chowdhury, D. J. Christopher, S. Dey, S. Fisher, B. Fraumeni, R. Fuller, A. G. Ghoshal, M. J. Golechha, P. C. Gupta, R. Gupta, R. Gupta, S. Gupta, S. Guttikunda, D. Hanrahan, S. Harikrishnan, P. Jeemon, T. K. Joshi, R. Kant, S. Kant, T. Kaur, P. A. Koul, P. Kumar, R. Kumar, S. L. Larson, R. Lodha, K. K. Madhipatla, P. A. Mahesh, R. Malhotra, S. Managi, K. Martin, M. Mathai, J. L. Mathew, R. Mehrotra, B. V. M. Mohan, V. Mohan, S. Mukhopadhyay, P. Mutreja, N. Naik, S. Nair, J. D. Pandian, P. Pant, A. Perianayagam, D. Prabhakaran, P. Prabhakaran, G. K. Rath, S. Ravi, A. Roy, Y. D. Sabde, S. Salvi, S. Sambandam, B. Sharma, M. Sharma, S. Sharma, R. S. Sharma, A. Shrivastava, S. Singh, V. Singh, R. Smith, J. D. Stanaway, G. Taghian, N. Tandon, J. S. Thakur, N. J. Thomas, G. S. Toteja, C. M. Varghese, C. Venkataraman, K. N. Venugopal, K. D. Walker, A. Y. Watson, S. Wozniak, D. Xavier, G. N. Yadama, G. Yadav, D. K. Shukla, H. J. Bekedam, K. S. Reddy, R. Guleria, T. Vos, S. S. Lim, R. Dandona, S. Kumar, P. Kumar, P. J. Landrigan, L. Dandona, Health and economic impact of air pollution in the states of India: The Global Burden of Disease Study 2019. *Lancet Planet. Health* **5**, e25–e38 (2021).
6. P. Rafaj, G. Kiesewetter, V. Krey, W. Schoepp, C. Bertram, L. Drouet, O. Fricko, S. Fujimori, M. Harmsen, J. Hilaire, D. Huppmann, Z. Klimont, P. Kolp, L. Aleluia Reis, D. van Vuuren, Air quality and health implications of 1.5°C–2°C climate pathways under considerations of ageing population: A multi-model scenario analysis. *Environ. Res. Lett.* **16**, 045005 (2021).
7. J. Sampedro, A. Markandya, C. Rodés-Bachs, D.-J. Van De Ven, Short-term health co-benefits of existing climate policies: The need for more ambitious and integrated policy action. *Lancet Planet. Health* **7**, e540–e541 (2023).
8. T. Vandyck, K. Keramidas, A. Kitous, J. V. Spadaro, R. van Dingenen, M. Holland, B. Saveyn, Air quality co-benefits for human health and agriculture counterbalance costs to meet Paris Agreement pledges. *Nat. Commun.* **9**, 4939 (2018).
9. S. Rao, Z. Klimont, S. J. Smith, R. van Dingenen, F. Dentener, L. Bouwman, K. Riahi, M. Amann, B. L. Bodirsky, D. P. van Vuuren, L. Aleluia Reis, K. Calvin, L. Drouet, O. Fricko, S. Fujimori, D. Gernaat, P. Havlik, M. Harmsen, T. Hasegawa, C. Heyes, J. Hilaire, G. Luderer, T. Masui, E. Stehfest, J. Strefler, S. van der Sluis, M. Tavoni, Future air pollution in the shared socio-economic pathways. *Global Environ. Chang* **42**, 346–358 (2017).
10. L. A. Reis, L. Drouet, M. Tavoni, Internalising health-economic impacts of air pollution into climate policy: A global modelling study. *Lancet Planet. Health* **6**, e40–e48 (2022).
11. K. Kuklinska, L. Wolska, J. Namiesnik, Air quality policy in the U.S. and the EU - A review. *Atmos. Pollut. Res.* **6**, 129–137 (2015).
12. A. Markandya, J. Sampedro, S. J. Smith, R. van Dingenen, C. Pizarro-Irizar, I. Arto, M. González-Eguino, Health co-benefits from air pollution and mitigation costs of the Paris Agreement: A modelling study. *Lancet Planet. Health* **2**, e126–e133 (2018).
13. S. Khomenko, M. Cirach, E. Pereira-Barboza, N. Mueller, J. Barrera-Gómez, D. Rojas-Rueda, K. de Hoogh, G. Hoek, M. Nieuwenhuijsen, Premature mortality due to air pollution in European cities: A health impact assessment. *Lancet Planet. Health* **5**, e121–e134 (2021).
14. L. A. Reis, L. Drouet, R. Dingenen, J. Emmerling, Future global air quality indices under different socioeconomic and climate assumptions. *Sustainability* **10**, 3645 (2018).
15. P. R. Shukla, J. Skea, R. Slade, A. Al Khourdajie, R. van Diemen, D. McCollum, J. Malley, *IPCC, 2022: Climate change 2022: Mitigation of climate change. Contribution of Working Group III to the Sixth Assessment Report of the Intergovernmental Panel on Climate Change.* (Cambridge Univ. Press, 2022); https://doi.org/10.1017/9781009157926.
16. J. Weyant, Some contributions of integrated assessment models of global climate change. *Rev. Environ. Econ. Policy* **11**, 115–137 (2017).
17. B. M. Sanderson, Y. Xu, C. Tebaldi, M. Wehner, B. O'Neill, A. Jahn, A. G. Pendergrass, F. Lehner, W. G. Strand, L. Lin, R. Knutti, J. F. Lamarque, Community climate simulations to assess avoided impacts in 1.5 and 2 °C futures. *Dynamics* **8**, 827–847 (2017).
18. T. Hasegawa, S. Fujimori, S. Frank, F. Humpenöder, C. Bertram, J. Després, L. Drouet, J. Emmerling, M. Gusti, M. Harmsen, K. Keramidas, Y. Ochi, K. Oshiro, P. Rochedo, B. van Ruijven, A. M. Cabardos, A. Deppermann, F. Fosse, P. Havlik, V. Krey, A. Popp, R. Schaeffer, D. van Vuuren, K. Riahi, Land-based implications of early climate actions without global net-negative emissions. *Nat. Sustain.* **4**, 1052–1059 (2021).

19. L. Drouet, V. Bosetti, S. A. Padoan, L. Aleluia Reis, C. Bertram, F. Dalla Longa, J. Després, J. Emmerling, F. Fosse, K. Fragkiadakis, S. Frank, O. Fricko, S. Fujimori, M. Harmsen, V. Krey, K. Oshiro, L. P. Nogueira, L. Paroussos, F. Piontek, K. Riahi, P. R. R. Rochedo, R. Schaeffer, J. Takakura, K. I. van der Wijst, B. van der Zwaan, D. van Vuuren, Z. Vrontisi, M. Weitzel, B. Zakeri, M. Tavoni, Net zero-emission pathways reduce the physical and economic risks of climate change. *Nat. Clim. Chang.* **11**, 1070–1076 (2021).
20. K. Tanaka, B. C. O'Neill, The Paris Agreement zero-emissions goal is not always consistent with the 1.5 °C and 2 °C temperature targets. *Nat. Clim. Chang.* **8**, 319–324 (2018).
21. K. Riahi, C. Bertram, D. Huppmann, J. Rogelj, V. Bosetti, A. M. Cabardos, A. Deppermann, L. Drouet, S. Frank, O. Fricko, S. Fujimori, M. Harmsen, T. Hasegawa, V. Krey, G. Luderer, L. Paroussos, R. Schaeffer, M. Weitzel, B. van der Zwaan, Z. Vrontisi, F. D. Longa, J. Després, F. Fosse, K. Fragkiadakis, M. Gusti, F. Humpenöder, K. Keramidas, P. Kishimoto, E. Kriegler, M. Meinshausen, L. P. Nogueira, K. Oshiro, A. Popp, P. R. R. Rochedo, G. Ünlü, B. van Ruijven, J. Takakura, M. Tavoni, D. van Vuuren, B. Zakeri, Cost and attainability of meeting stringent climate targets without overshoot. *Nat. Clim. Chang.* **11**, 1063–1069 (2021).
22. E. Byers, V. Krey, E. Kriegler, K. Riahi, R. Schaeffer, J. Kikstra, R. Lamboll, Z. Nicholls, M. Sandstad, C. Smith, K. V. der Wijst, A. Al -Khourdajie, F. Lecocq, J. Portugal-Pereira, Y. Saheb, A. Stromman, H. Winkler, C. Auer, E. Brutschin, M. Gidden, AR6 Scenarios Database (2022); https://doi.org/10.5281/zenodo.7197970.
23. S. Fujimori, T. Hasegawa, T. Masui, K. Takahashi, Land use representation in a global CGE model for long-term simulation: CET vs. logit functions. *Food Secur.* **6**, 685–699 (2014).
24. S. Fujimori, T. Masui, Y. Matsuoka, "AIM/CGE [basic] manual," *Discussion Paper Series* (no. 2012-01) (2012).
25. E. Stehfest, D. van Vuuren, L. Bouwman, T. Kram, "Integrated assessment of global environmental change with IMAGE 3.0 - Model description and policy applications" (PBL Netherlands Environmental Assessment Agency, 2014).
26. D. Huppmann, M. Gidden, O. Fricko, P. Kolp, C. Orthofer, M. Pimmer, N. Kushin, A. Vinca, A. Mastrucci, K. Riahi, V. Krey, The MESSAGE Integrated Assessment Model and the ix modeling platform (ixmp): An open framework for integrated and cross-cutting analysis of energy, climate, the environment, and sustainable development. *Environ. Model. Softw.* **112**, 143–156 (2019).
27. J. Després, K. Keramidas, A. Schmitz, A. Kitous, B. Schade, A. R. Diaz-Vazquez, S. Mima, H. P. Russ, T. Wiesenthal, "POLES-JRC model documentation - Updated for 2018" (JRC113757, Publications Office of the European Union, 2018).
28. E. Kriegler, N. Bauer, A. Popp, F. Humpenöder, M. Leimbach, J. Strefler, L. Baumstark, B. L. Bodirsky, J. Hilaire, D. Klein, I. Mouratiadou, I. Weindl, C. Bertram, J. P. Dietrich, G. Luderer, M. Pehl, R. Pietzcker, F. Piontek, H. Lotze-Campen, A. Biewald, M. Bonsch, A. Giannousakis, U. Kreidenweis, C. Müller, S. Rolinski, A. Schultes, J. Schwanitz, M. Stevanovic, K. Calvin, J. Emmerling, S. Fujimori, O. Edenhofer, Fossil-fueled development (SSP5): An energy and resource intensive scenario for the 21st century. *Global Environ. Chang.* **42**, 297–315 (2017).
29. G. Luderer, R. C. Pietzcker, C. Bertram, E. Kriegler, M. Meinshausen, O. Edenhofer, Economic mitigation challenges: How further delay closes the door for achieving climate targets. *Environ. Res. Lett.* **8**, 034033 (2013).
30. V. Bosetti, M. Galeotti, M. Tavoni, C. Carraro, E. Massetti, Witch a world induced technical change hybrid model. *Energy J. Hybrid Model.* **27**, 13–37 (2006).
31. J. Emmerling, L. A. Reis, M. Bevione, L. Berger, V. Bosetti, S. Carrara, G. Marangoni, F. Sferra, M. Tavoni, J. Witajewski-Baltvilks, P. Havllk, The WITCH 2016 Model - Documentation and implementation of the shared socioeconomic pathways. *FEEM Working paper* **42**, 10.2139/ssrn.2800970 (2016).
32. L. Braunreiter, L. van Beek, M. Hajer, D. van Vuuren, Transformative pathways - Using integrated assessment models more effectively to open up plausible and desirable low-carbon futures. *Energy Res. Soc. Sci.* **80**, 102220 (2021).
33. D.-J. van de Ven, S. Mittal, A. Gambhir, R. D. Lamboll, H. Doukas, S. Giarola, A. Hawkes, K. Koasidis, A. C. Köberle, H. M. Jeon, S. Perdana, G. P. Peters, J. Rogelj, I. Sognnaes, M. Vielle, A. Nikas, A multimodel analysis of post-Glasgow climate targets and feasibility challenges. *Nat. Clim. Chang.* **13**, 570–578 (2023).
34. M. C. Bryson, Heavy-tailed distributions: Properties and tests. *Technometrics* **16**, 61–68 (1974).
35. K. Riahi, B. Christoph, L. Drouet, T. Hasegawa, F. D. Longa, J. Desprès, F. Fosse, K. Fragkiadakis, O. Fricko, M. Gusti, F. Humpenöder, K. Keramidas, P. Kishimoto, E. Kriegler, L. P. Nogueira, K. Oshiro, A. Popp, P. R. R. Rochedo, J. Takakura, G. Ünlü, B. van Ruijven, D. van Vuuren, B. Zakeri, V. Bosetti, A.-M. Cabardos, A. Deppermann, Harmen-Sytze de Boer, J. Emmerling, S. Frank, S. Fujimori, M. Harmsen, P. Havlik, J. Hilaire, D. Huppmann, K. Keramidas, V. Krey, G. Luderer, A. Malik, M. Meinshausen, Y. Ochi, L. Paroussos, J. Rogelj, D. Saygin, R. Schaeffer, M. Tavoni, B. van der Zwaan, Z. Vrontisi, M. Weitzel, ENGAGE Global Scenarios (2021); https://zenodo.org/record/5078071.
36. C. A. Belis, D. Pernigotti, G. Pirovano, O. Favez, J. L. Jaffrezo, J. Kuenen, H. Denier van der Gon, M. Reizer, V. Riffault, L. Y. Alleman, M. Almeida, F. Amato, A. Angyal, G. Argyropoulos, S. Bande, I. Beslic, J. L. Besombes, M. C. Bove, P. Brotto, G. Calori, D. Cesari, C. Colombi, D. Contini, G. de Gennaro, A. di Gilio, E. Diapouli, I. el Haddad, H. Elbern, K. Eleftheriadis, J. Ferreira, M. G. Vivanco, S. Gilardoni, B. Golly, S. Hellebust, P. K. Hopke, Y. Izadmanesh, H. Jorquera, K. Krajsek, R. Kranenburg, P. Lazzeri, F. Lenartz, F. Lucarelli, K. Maciejewska, A. Manders, M. Manousakas, M. Masiol, M. Mircea, D. Mooibroek, S. Nava, D. Oliveira, M. Paglione, M. Pandolfi, M. Perrone, E. Petralia, A. Pietrodangelo, S. Pillon, P. Pokorna, P. Prati, D. Salameh, C. Samara, L. Samek, D. Saraga, S. Sauvage, M. Schaap, F. Scotto, K. Sega, G. Siour, R. Tauler, G. Valli, R. Vecchi, E. Venturini, M. Vestenius, A. Waked, E. Yubero, Evaluation of receptor and chemical transport models for PM10 source apportionment. *Atmos. Environ. X* **5**, 100053 (2020).
37. A. Sayeed, E. Eslami, Y. Lops, Y. Choi, CMAQ-CNN: A new-generation of post-processing techniques for chemical transport models using deep neural networks. *Atmos. Environ.* **273**, 118961 (2022).
38. R. V. Dingenen, F. Dentener, M. Crippa, J. Leitao, E. Marmer, S. Rao, E. Solazzo, L. Valentini, TM5-FASST: A global atmospheric source-receptor model for rapid impact analysis of emission changes on air quality and short-lived climate pollutants. *Atmos. Chem. Phys.* **18**, 16173–16211 (2018).
39. W. Chen, X. Lu, D. Yuan, Y. Chen, Z. Li, Y. Huang, T. Fung, H. Sun, J. C. H. Fung, Global PM2.5Prediction and associated mortality to 2100 under different climate change scenarios. *Environ. Sci. Technol.* **57**, 10039–10052 (2023).
40. L. Ciao-Kai, J. J. West, R. A. Silva, H. Bian, M. Chin, Y. Davila, F. J. Dentener, L. Emmons, J. Flemming, G. Folberth, D. Henze, U. Im, J. E. Jonson, T. J. Keating, T. Kucsera, A. Lenzen, M. Lin, M. T. Lund, X. Pan, R. J. Park, R. B. Pierce, T. Sekiya, K. Sudo, T. Takemura, HTAP2 multi-model estimates of premature human mortality due to intercontinental transport of air pollution and emission sectors. *Atmos. Chem. Phys.* , 10497–10520 (2018).
41. M. Jerrett, R. T. Burnett, C. A. Pope III, K. Ito, G. Thurston, D. Krewski, Y. Shi, E. Calle, M. Thun, Long-term ozone exposure and mortality. *N. Eng. J. Med.* **360**, 1085–1095 (2009).
42. J. Lelieveld, J. S. Evans, M. Fnais, D. Giannadaki, A. Pozzer, The contribution of outdoor air pollution sources to premature mortality on a global scale. *Nature* **525**, 367–371 (2015).
43. OECD, *Mortality Risk Valuation in Environment, Health and Transport Policies* (OECD Publishing) (2012); https://doi.org/10.1787/9789264130807-en.
44. L. A. Parsons, D. Shindell, G. Faluvegi, E. Nagamoto, Geophysical uncertainties in air pollution exposure and benefits of emissions reductions for global health. *Earths Future* **11**, e2023EF003839 (2023).
45. F. C. Moore, D. B. Diaz, Temperature impacts on economic growth warrant stringent mitigation policy. *Nat. Clim. Chang.* **5**, 127–131 (2015).
46. A. van Donkelaar, M. S. Hammer, L. Bindle, M. Brauer, J. R. Brook, M. J. Garay, N. C. Hsu, O. V. Kalashnikova, R. A. Kahn, C. Lee, R. C. Levy, A. Lyapustin, A. M. Sayer, R. V. Martin, Monthly global estimates of fine particulate matter and their uncertainty. *Environ. Sci. Technol.* **55**, 15287–15300 (2021).
47. J. D. Gibbons, S. Chakraborti, *Nonparametric Statistical Inference* (Springer, 2011).
48. R. Beelen, O. Raaschou-Nielsen, M. Stafoggia, Z. J. Andersen, G. Weinmayr, B. Hoffmann, K. Wolf, E. Samoli, P. Fischer, M. Nieuwenhuijsen, P. Vineis, W. W. Xun, K. Katsouyanni, K. Dimakopoulou, A. Oudin, B. Forsberg, L. Modig, A. S. Havulinna, T. Lanki, A. Turunen, B. Oftedal, W. Nystad, P. Nafstad, U. De Faire, N. L. Pedersen, C.-G. Östenson, L. Fratiglioni, J. Penell, M. Korek, G. Pershagen, K. T. Eriksen, K. Overvad, T. Ellermann, M. Eeftens, P. H. Peeters, K. Meliefste, M. Wang, B. Bueno-de-Mesquita, D. Sugiri, U. Krämer, J. Heinrich, K. de Hoogh, T. Key, A. Peters, R. Hampel, H. Concin, G. Nagel, A. Ineichen, E. Schaffner, N. Probst-Hensch, N. Künzli, C. Schindler, T. Schikowski, M. Adam, H. Phuleria, A. Vilier, F. Clavel-Chapelon, C. Declercq, S. Grioni, V. Krogh, M.-Y. Tsai, F. Ricceri, C. Sacerdote, C. Galassi, E. Migliore, A. Ranzi, G. Cesaroni, C. Badaloni, F. Forastiere, I. Tamayo, P. Amiano, M. Dorronsoro, M. Katsoulis, A. Trichopoulou, B. Brunekreef, G. Hoek, Effects of long-term exposure to air pollution on natural-cause mortality: An analysis of 22 European cohorts within the multicentre ESCAPE project. *Lancet* **383**, 785–795 (2013).
49. R. Burnett, H. Chen, M. Szyszkowicz, N. Fann, B. Hubbell, C. A. Pope III, J. S. Apte, M. Brauer, A. Cohen, S. Weichenthal, J. Coggins, Q. di, B. Brunekreef, J. Frostad, S. S. Lim, H. Kan, K. D. Walker, G. D. Thurston, R. B. Hayes, C. C. Lim, M. C. Turner, M. Jerrett, D. Krewski, S. M. Gapstur, W. R. Diver, B. Ostro, D. Goldberg, D. L. Crouse, R. V. Martin, P. Peters, L. Pinault, M. Tjepkema, A. van Donkelaar, P. J. Villeneuve, A. B. Miller, P. Yin, M. Zhou, L. Wang, N. A. H. Janssen, M. Marra, R. W. Atkinson, H. Tsang, T. Quoc Thach, J. B. Cannon, R. T. Allen, J. E. Hart, F. Laden, G. Cesaroni, F. Forastiere, G. Weinmayr, A. Jaensch, G. Nagel, H. Concin, J. V. Spadaro, Global estimates of mortality associated with long-term exposure to outdoor fine particulate matter. *Proc. Natl. Acad. Sci. U.S.A.* **115**, 9592–9597 (2018).
50. R. Burnett, C. A. Pope III, M. Ezzati, C. Olives, S. S. Lim, S. Mehta, H. H. Shin, G. Singh, B. Hubbell, M. Brauer, H. R. Anderson, K. R. Smith, J. R. Balmes, N. G. Bruce, H. Kan, F. Laden, A. Prüss-Ustün, M. C. Turner, S. M. Gapstur, W. R. Diver, A. Cohen, An integrated risk function for estimating the global burden of disease attributable to ambient fine particulate matter exposure. *Environ. Health Perspect.* **122**, 397–403 (2014).
51. A. Cohen, H. Ross Anderson, B. Ostro, K. D. Pandey, M. Krzyzanowski, N. Künzli, K. Gutschmidt, A. Pope, I. Romieu, J. M. Samet, K. Smith, The global burden of disease due to outdoor air pollution. *J. Toxicol. Environ. Health A* **68**, 1301–1307 (2005).

52. M. Ezzati, A. D. Lopez, A. Rodgers, C. J. Murray, *Comparative Quantification of Health Risks: Global and Regional Burden of Disease Attributable to Selected Major Risk Factors* (World Health Organization Geneva, 2004), vol. 2, pp. 1353–1433.
53. M. Nasari, M. Szyszkowicz, H. Chen, D. Crouse, M. C. Turner, M. Jerrett, C. A. Pope III, B. Hubbell, N. Fann, A. Cohen, S. M. Gapstur, W. R. Diver, D. Stieb, M. H. Forouzanfar, S. Y. Kim, C. Olives, D. Krewski, R. T. Burnett, A class of non-linear exposure-response models suitable for health impact assessment applicable to large cohort studies of ambient air pollution. *Air Qual. Atmos. Health* **9**, 961–972 (2016).
54. C. A. Pope III, R. T. Burnett, M. J. Thun, E. E. Calle, D. Krewski, K. Ito, G. D. Thurston, Lung cancer, cardiopulmonary mortality, and long-term exposure to fine particulate air pollution. *JAMA* **287**, 1132–1141 (2002).
55. K. S. Reddy, Global Burden of Disease Study 2015 provides GPS for global health 2030. *Lancet* **388**, 1448–1449 (2016).
56. F. Piontek, M. Kalkuhl, E. Kriegler, A. Schultes, M. Leimbach, O. Edenhofer, N. Bauer, Economic growth effects of alternative climate change impact channels in economic modeling. *Environ. Resour. Econ.* **73**, 1357–1385 (2019).
57. R. S. J. Tol, "The economic impacts of climate change," in *Review of Environmental Economics and Policy* (The University of Chicago Press, 2018).
58. A. Dechezleprêtre, N. Rivers, B. Stadler, "The economic cost of air pollution: Evidence from Europe," *OECD Economics Department Working Papers* (no. 1584) (OECD Publishing, 2019); www.oecd.org/en/publications/the-economic-cost-of-air-pollution-evidence-from-europe_56119490-en.html.
59. D. Dong, X. Boyang, S. Ning, H. Qian, The adverse impact of air pollution on China's economic growth. *Sustainability* **13**, 9056 (2021).
60. W. Zhang, J. Zhao, Z. Zhang, M. Liu, R. Li, W. Xue, J. Xing, B. Cai, L. Jiang, J. Zhang, X. Hu, L. Zhong, H. Jiang, J. Wang, J. Bi, The economy-employment-environmental health transfer and embedded inequities of China's capital metropolitan area: A mixed-methods study. *Lancet Planet. Health* **7**, e912–e924 (2023).
61. A. Nikas, A. Gambhir, E. Trutnevyte, K. Koasidis, H. Lund, J. Z. Thellufsen, D. Mayer, G. Zachmann, L. J. Miguel, N. Ferreras-Alonso, I. Sognnaes, G. P. Peters, E. Colombo, M. Howells, A. Hawkes, M. van den Broek, D. J. van de Ven, M. Gonzalez-Eguino, A. Flamos, H. Doukas, Perspective of comprehensive and comprehensible multi-model energy and climate science in Europe. *Energy* **215**, 119153 (2021).
62. C. Guivarch, T. le Gallic, N. Bauer, P. Fragkos, D. Huppmann, M. Jaxa-Rozen, I. Keppo, E. Kriegler, T. Krisztin, G. Marangoni, S. Pye, K. Riahi, R. Schaeffer, M. Tavoni, E. Trutnevyte, D. van Vuuren, F. Wagner, Using large ensembles of climate change mitigation scenarios for robust insights. *Nat. Clim. Chang.* **12**, 428–435 (2022).
63. B. Zhao, S. Wang, J. Hao, Challenges and perspectives of air pollution control in China. *Front. Environ. Sci. Eng.* **18**, 68 (2024).
64. K. Balakrishnan, S. Dey, T. Gupta, R. S. Dhaliwal, M. Brauer, A. J. Cohen, J. D. Stanaway, G. Beig, T. K. Joshi, A. N. Aggarwal, Y. Sabde, H. Sadhu, J. Frostad, K. Causey, W. Godwin, D. K. Shukla, G. A. Kumar, C. M. Varghese, P. Muraleedharan, A. Agrawal, R. M. Anjana, A. Bhansali, D. Bhardwaj, K. Burkart, K. Cercy, J. K. Chakma, S. Chowdhury, D. J. Christopher, E. Dutta, M. Furtado, S. Ghosh, A. G. Ghoshal, S. D. Glenn, R. Guleria, R. Gupta, P. Jeemon, R. Kant, S. Kant, T. Kaur, P. A. Koul, V. Krish, B. Krishna, S. L. Larson, K. Madhipatla, P. A. Mahesh, V. Mohan, S. Mukhopadhyay, P. Mutreja, N. Naik, S. Nair, G. Nguyen, C. M. Odell, J. D. Pandian, D. Prabhakaran, P. Prabhakaran, A. Roy, S. Salvi, S. Sambandam, D. Saraf, M. Sharma, A. Shrivastava, V. Singh, N. Tandon, N. J. Thomas, A. Torre, D. Xavier, G. Yadav, S. Singh, C. Shekhar, T. Vos, R. Dandona, K. S. Reddy, S. S. Lim, C. J. L. Murray, S. Venkatesh, L. Dandona, The impact of air pollution on deaths, disease burden, and life expectancy across the states of India: The Global Burden of Disease Study 2017. *Lancet Planet. Health* **3**, e26–e39 (2019).
65. United Nations, Paris Agreement to the United Nations Framework Convention on Climate Change (2015); https://unfccc.int/sites/default/files/english_paris_agreement.pdf.
66. Institute for Health Metrics and Evaluation, IHME-GBD Database; https://vizhub.healthdata.org/gbd-results/ [accessed March 2025].
67. GBD 2019 Diseases and Injuries Collaborators, Global burden of 369 diseases and injuries in 204 countries and territories, 1990–2019: A systematic analysis for the Global Burden of Disease Study 2019. *Lancet* **396**, 1204–1222 (2020).
68. N. Paisi, J. Kushta, A. Pozzer, A. Violaris, J. Lelieveld, Health effects of carbonaceous PM2. 5 compounds from residential fuel combustion and road transport in Europe. *Sci. Rep.* **14**, 1530 (2024).
69. A. Pozzer, S. C. Anenberg, S. Dey, A. Haines, J. Lelieveld, S. Chowdhury, Mortality attributable to ambient air pollution: A review of global estimates. *GeoHealth* **7**, e2022GH000711 (2023).
70. Health Effects Institute, "State of global air 2020" (Special Report, Health Effects Institute, 2020).
71. GBD 2019 Risk Factors Collaborators, Global burden of 87 risk factors in 204 countries and territories, 1990–2019: A systematic analysis for the Global Burden of Disease Study 2019. *Lancet* **396**, 1223–1249 (2020).
72. J. G. Ayres, "The mortality effects of long-term exposure to particulate air pollution in the United Kingdom" (Tech. Rep., Health Protection Agency for the Committee on the Medical Effects of Air Pollutants, 2010).
73. M. A. Mansournia, D. G. Altman, Population attributable fraction. *BMJ* **360**, k757 (2018).
74. S. Anenberg, L. Horowitz, D. Tong, J. West, An estimate of the global burden of anthropogenic ozone and fine particulate matter on premature human mortality using atmospheric modeling. *Environ. Health Perspect.* **118**, 1189–1195 (2010).
75. World Health Organization, Global Health Observatory Resources; www.who.int/data/gho/indicator-metadata-registry.
76. S. S. Lim, T. Vos, A. D. Flaxman, G. Danaei, K. Shibuya, H. Adair-Rohani, M. Amann, H. R. Anderson, K. G. Andrews, M. Aryee, C. Atkinson, L. J. Bacchus, A. N. Bahalim, K. Balakrishnan, J. Balmes, S. Barker-Collo, A. Baxter, M. L. Bell, J. D. Blore, F. Blyth, C. Bonner, G. Borges, R. Bourne, M. Boussinesq, M. Brauer, P. Brooks, N. G. Bruce, B. Brunekreef, C. Bryan-Hancock, C. Bucello, R. Buchbinder, F. Bull, R. T. Burnett, T. E. Byers, B. Calabria, J. Carapetis, E. Carnahan, Z. Chafe, F. Charlson, H. Chen, J. S. Chen, A. T.-A. Cheng, J. C. Child, A. Cohen, K. E. Colson, B. C. Cowie, S. Darby, S. Darling, A. Davis, L. Degenhardt, F. Dentener, D. C. Des Jarlais, K. Devries, M. Dherani, E. L. Ding, E. R. Dorsey, T. Driscoll, K. Edmond, S. E. Ali, R. E. Engell, P. J. Erwin, S. Fahimi, G. Falder, F. Farzadfar, A. Ferrari, M. M. Finucane, S. Flaxman, F. G. R. Fowkes, G. Freedman, M. K. Freeman, E. Gakidou, S. Ghosh, E. Giovannucci, G. Gmel, K. Graham, R. Grainger, B. Grant, D. Gunnell, H. R. Gutierrez, W. Hall, H. W. Hoek, A. Hogan, H. D. Hosgood III, D. Hoy, H. Hu, B. J. Hubbell, S. J. Hutchings, S. E. Ibeanusi, G. L. Jacklyn, R. Jasrasaria, J. B. Jonas, H. Kan, J. A. Kanis, N. Kassebaum, N. Kawakami, Y.-H. Khang, S. Khatibzadeh, J.-P. Khoo, C. Kok, F. Laden, R. Lalloo, Q. Lan, T. Lathlean, J. L. Leasher, J. Leigh, Y. Li, J. K. Lin, S. E. Lipshultz, S. London, R. Lozano, Y. Lu, J. Mak, R. Malekzadeh, L. Mallinger, W. Marcenes, L. March, R. Marks, R. Martin, P. M. Gale, J. M. Grath, S. Mehta, G. A. Mensah, T. R. Merriman, R. Micha, C. Michaud, V. Mishra, K. M. Hanafiah, A. A. Mokdad, L. Morawska, D. Mozaffarian, T. Murphy, M. Naghavi, B. Neal, P. K. Nelson, J. M. Nolla, R. Norman, C. Olives, S. B. Omer, J. Orchard, R. Osborne, B. Ostro, A. Page, K. D. Pandey, C. D. H. Parry, E. Passmore, J. Patra, N. Pearce, P. M. Pelizzari, M. Petzold, M. R. Phillips, D. Pope, C. A. Pope III, J. Powles, M. Rao, H. Razavi, E. A. Rehfuess, J. T. Rehm, B. Ritz, F. P. Rivara, T. Roberts, C. Robinson, J. A. Rodriguez-Portales, I. Romieu, R. Room, L. C. Rosenfeld, A. Roy, L. Rushton, J. A. Salomon, U. Sampson, L. Sanchez-Riera, E. Sanman, A. Sapkota, S. Seedat, P. Shi, K. Shield, R. Shivakoti, G. M. Singh, D. A. Sleet, E. Smith, K. R. Smith, N. J. C. Stapelberg, K. Steenland, H. Stöckl, L. J. Stovner, K. Straif, L. Straney, G. D. Thurston, J. H. Tran, R. Van Dingenen, A. van Donkelaar, J. L. Veerman, L. Vijayakumar, R. Weintraub, M. M. Weissman, R. A. White, H. Whiteford, S. T. Wiersma, J. D. Wilkinson, H. C. Williams, W. Williams, N. Wilson, A. D. Woolf, P. Yip, J. M. Zielinski, A. D. Lopez, C. J. L. Murray, M. Ezzati, M. A. Al Mazroa, Z. A. Memish, A comparative risk assessment of burden of disease and injury attributable to 67 risk factors and risk factor clusters in 21 regions, 1990–2010: A systematic analysis for the Global Burden of Disease Study 2010. *Lancet* **380**, 2224–2260 (2012).
77. D. Krewski, M. Jerrett, R. T. Burnett, R. Ma, E. Hughes, Y. Shi, M. C. Turner, C. A. Pope III, G. Thurston, E. E. Calle, M. J. Thun, B. Beckerman, P. DeLuca, N. Finkelstein, K. Ito, D. K. Moore, K. B. Newbold, T. Ramsay, Z. Ross, H. Shin, B. Tempalski, Extended follow-up and spatial analysis of the american cancer society study linking particulate air pollution and mortality. *Res. Rep. Health Eff. Inst.* **140**, 5–114 (2009).
78. R. Burnett, A. Cohen, Relative risk functions for estimating excess mortality attributable to outdoor PM2.5 air pollution: Evolution and state-of-the-art. *Atmosphere* **11**, 589 (2020).
79. A. Cohen, M. Brauer, R. Burnett, H. R. Anderson, J. Frostad, K. Estep, K. Balakrishnan, B. Brunekreef, L. Dandona, R. Dandona, V. Feigin, G. Freedman, B. Hubbell, A. Jobling, H. Kan, L. Knibbs, Y. Liu, R. Martin, L. Morawska, C. A. Pope III, H. Shin, K. Straif, G. Shaddick, M. Thomas, R. van Dingenen, A. van Donkelaar, T. Vos, C. J. L. Murray, M. H. Forouzanfar, Estimates and 25-year trends of the global burden of disease attributable to ambient air pollution: An analysis of data from the Global Burden of Diseases Study 2015. *Lancet* **389**, 1907–1918 (2017).
80. P. Fantke, T. E. McKone, M. Tainio, O. Jolliet, J. S. Apte, K. S. Stylianou, N. Illner, J. D. Marshall, E. F. Choma, J. S. Evans, Global effect factors for exposure to fine particulate matter. *Environ. Sci. Technol.* **53**, 6855–6868 (2019).
81. Public Health, Social and Enviromental Determinants of Health Department, World Health Organization, "Burden of disease from the joint effects of household and ambient Air pollution for 2016," *Global Health Estimates Technical Paper* (2018); www.biomassmurder.org/docs/2018-05-00-world-health-organization-report-burden-of-disease-from-ambient-air-pollution-for-2016-english.pdf.
82. GBD 2017 Risk Factor Collaborators, Global, regional, and national comparative risk assessment of 84 behavioural, environmental and occupational, and metabolic risks or clusters of risks for 195 countries and territories, 1990–2017: A systematic analysis for the Global Burden of Disease Study 2017. *Lancet* **392**, 1923–1994 (2017).
83. World Health Organization, "Health risks of air pollution in Europe - HRAPIE project - Recommendations for concentration-response functions for cost-benefit analysis of particulate matter, ozone, and nitrogen dioxide" (WHO Regional Office for Europe, 2013); https://iris.who.int/handle/10665/153692.
84. Global Energy Assessment, *Global Energy Assessment - Toward a Sustainable Future* (Cambridge Univ. Press and the International Institute for Applied Systems Analysis, 2012); www.globalenergyassessment.org.

85. United Nations Department of Economic and Social Affairs (UN DESA), "World population prospects: The 2008 revision database," Working paper, United Nations Department of Economic and Social Affairs (UN DESA), New York, 2008.
86. R. Roy, D. Weis, F. George, *Economic Cost of the Health Impact of Air Pollution in Europe: Clean Air, Health and Wealth* (World Health Organization, Regional Office for Europe, 2015).
87. L. A. Robinson, J. K. Hammitt, L. O'Keeffe, Valuing mortality risk reductions in global benefit-cost analysis. *J. Benefit Cost Anal.* **10**, 15–50 (2019).
88. X. Zhao, S. Huang, J. Wang, S. Kaiser, X. Han, The impacts of air pollution on human and natural capital in China: A look from a provincial perspective. *Ecol. Indic.* **118**, 106759 (2020).
89. G. Liu, Z. Yang, B. Chen, S. Ulgiati, Monitoring trends of urban development and environmental impact of Beijing, 1999–2006. *Sci. Total Environ.* **409**, 3295–3308 (2011).
90. K. Calvin, P. Patel, L. Clarke, G. Asrar, B. Bond-Lamberty, R. Y. Cui, A. di Vittorio, K. Dorheim, J. Edmonds, C. Hartin, M. Hejazi, R. Horowitz, G. Iyer, P. Kyle, S. Kim, R. Link, H. McJeon, S. J. Smith, A. Snyder, S. Waldhoff, M. Wise, GCAM v5.1: Representing the linkages between energy, water, land, climate, and economic systems. *Geosci. Model Dev.* **12**, 677–698 (2019).
91. W. K. Viscusi, C. J. Masterman, Income elasticities and global values of a statistical life. *J. Benefit Cost Anal.* **8**, 226–250 (2017).
92. S. Chattopadhyay, *Education and Economics: Disciplinary Evolution and Policy Discourse* (Oxford Univ. Press, 2012).
93. S. Foss, D. Korshunov, S. Zachary, "Heavy-tailed and long-tailed distributions," in *An Introduction to Heavy-Tailed and Subexponential Distributions* (Springer, 2013), pp. 7–42.
94. L. d. Haan, A. Ferreira, *Extreme Value Theory: An Introduction*, Springer series in Operations Research and Financial Engineering (Springer, 2006).
95. A. Agresti, B. A. Coull, Approximate is better than "exact" for interval estimation of binomial proportions. *Am. Stat.* **52**, 119–126 (1998).
96. H Abdi, *Binomial Test*, The Concise Encyclopedia of Statistics (Springer, 2008).

Acknowledgments
Funding: This work was funded by the European Union's Horizon Europe Research and Innovation Program under the ENGAGE project (grant number 821471), AdJUST (Advancing the understanding of challenges, policy options and measures to achieve a JUST EU energy transition) project (grant number 101069880), and the GRINS (Growing Resilient, INclusive and Sustainable) project (grant number PE00000018). **Author contributions:** Conceptualization: C.R.-B., L.A.R., L.D., and M.T. Methodology: C.R.-B., L.A.R., and L.D. Investigation: C.R.-B., L.A.R., and L.D. Visualization: C.R.-B. and L.A.R. Supervision: L.A.R. Writing—original draft: C.R.-B. Writing—review and editing: C.R.-B., L.A.R., L.D., M.T., and P.R. **Competing interests:** The authors declare that they have no competing interests. **Data and materials availability:** The global climate change mitigation scenario dataset analyzed in this study is available in Zenodo at https://doi.org/10.5281/zenodo.16266654. All other data needed to evaluate the conclusions of the paper are present in the paper and/or the Supplementary Materials. The source code used for the data analysis and the figure generation, both for the manuscript and the Supplementary Materials, can be found in the online repository https://github.com/klau506/AP_overshoot_damages and https://zenodo.org/records/16266654.

Submitted 20 November 2024
Accepted 12 September 2025
Published 17 October 2025
10.1126/sciadv.adu7590

ScienceAdvances

Beyond the limit: The estimated air pollution damages of overshooting the temperature target

Clàudia Rodés-Bachs, Laurent Drouet, Peter Rafaj, Massimo Tavoni, and Lara Aleluia Reis

Sci. Adv. **11** (42), eadu7590. DOI: 10.1126/sciadv.adu7590